Three-dimensional geologic map of the Hayward fault, northern California: Correlation of rock units with variations in seismicity, creep rate, and fault dip

R.W. Graymer
D.A. Ponce
R.C. Jachens
R.W. Simpson
G.A. Phelps
C.M. Wentworth

U.S. Geological Survey, 345 Middlefield Road, Menlo Park, California 94025, USA

ABSTRACT

In order to better understand mechanisms of active faults, we studied relationships between fault behavior and rock units along the Hayward fault using a three-dimensional geologic map. The three-dimensional map—constructed from hypocenters, potential field data, and surface map data—provided a geologic map of each fault surface, showing rock units on either side of the fault truncated by the fault. The two fault-surface maps were superimposed to create a rock-rock juxtaposition map. The three maps were compared with seismicity, including aseismic patches, surface creep, and fault dip along the fault, by using visualization software to explore three-dimensional relationships. Fault behavior appears to be correlated to the fault-surface maps, but not to the rock-rock juxtaposition map, suggesting that properties of individual wall-rock units, including rock strength, play an important role in fault behavior. Although preliminary, these results suggest that any attempt to understand the detailed distribution of earthquakes or creep along a fault should include consideration of the rock types that abut the fault surface, including the incorporation of observations of physical properties of the rock bodies that intersect the fault at depth.

Keywords: Hayward fault, three-dimensional model, geologic map, faults, faulting, creep, relocated hypocenters.

INTRODUCTION

The Hayward fault (Fig. 1), part of the San Andreas fault system, roughly bisects the San Francisco Bay region, a densely populated area of about seven million people. This fault, which generated a severely damaging (M 6.8) earthquake in 1868, and its northern extension, the Rodgers Creek fault, are regarded as the most hazardous faults in the San Francisco Bay area with a probability of ~27% for an earthquake having $M \geq 6.7$ over the next 30 yr (Working Group on California Earthquake Probabilities, 2003). The high density of structures and lifelines along the Hayward fault make this a very dangerous fault, with the highest potential earthquake loss in the region and possibly in the United States.

The Hayward fault is the active part of a broader zone of faults ~1–5 km wide (Graymer et al., 1995) that forms the structural boundary between the allochthonous Franciscan Complex rocks underlying the San Francisco Bay plain and the parautochthonous Coast Range ophiolite and Great Valley Sequence rocks underlying the East Bay Hills. In the vicinity of the Hayward fault, the Franciscan Complex is composed of several distinct tectonostratigraphic terranes that include bedded sandstone and shale, melánge, and metagraywacke (Blake et al., 2002; Graymer, 2000; Graymer et al., 2002a). The broad fault zone has accumulated ~100 km of right-lateral slip since 12 Ma (Graymer et al., 2002b).

The active Hayward fault has a Quaternary geologic slip rate of ~9 mm/yr. The main surface trace, which is within the long-term fault zone, is creeping along most of its length at ~3.5–6 mm/yr, excluding high creep rates at Fremont (Lienkaemper et al., 2001). The hills east of the fault are rising, locally as fast as 1.5 mm/yr since 20 ka (Gilmore, 1992; Kelson and Simpson, 1995; Lienkaemper and Borchardt, 1996), suggesting that the active fault includes a reverse component.

Both the geologic units truncated and the fault character, including seismicity, creep rate, and fault dip, vary along the length of the Hayward fault. To understand the role of geology, specifically the three-dimensional (3-D) distribution of materials and structures surrounding the fault, we generated the first 3-D geologic map of the Hayward fault and its adjacent rock bodies. From that we derived geologic maps of the fault faces, as well as a rock-on-rock map of the juxtapositions across the fault. We discuss correlations of the derived maps with fault behavior and potential implications for studies of faults in general.

3-D GEOLOGIC MODEL AND GEOLOGIC MAPS OF THE FAULT FACES

A 3-D geologic map (Fig. 2) was assembled using EarthVision, a 3-D modeling package. EarthVision uses faults to subdivide a study volume into fault blocks, which can be further subdivided into stratigraphic units with depositional surfaces. The methods used to generate fault and depositional surfaces are described in the following.

Hypocenters

The primary active fault surface was derived from the mapped surface trace of the Hayward fault (Lienkaemper, 1992) and double-difference relocated earthquake hypocenters by manually fitting a downward projection of the surface trace through the hypocenters on cross sections oriented normal to the average fault trend and spaced 2.5 km apart (Ponce et al., 2004). A 3-D surface was then constructed through the cross-sectional traces and smoothed.

The relocated hypocenters are estimated to have relative location errors of ~100 m horizontally and 250 m vertically, and potentially much larger absolute location errors. Nevertheless, they represent the best data set related to the shape and position of the active fault at depth available as we constructed the 3-D map. The surface Hayward fault is a complex zone varying from perhaps a few hundred meters to several kilometers in width. However, at depth coseismic shearing on faults may be commonly restricted to zones <10 cm wide throughout the seismogenic zone (Sibson, 2003), so there a single plane may be a close approximation.

Potential Field Data

A 35 km stretch of the Hayward fault bisects a dense and magnetic ophiolitic body, much of it composed of gabbro. The subsurface extent and orientation of the gabbro were derived in the 3-D geologic map from analysis of gravity and aeromagnetic data (Ponce et al., 2003).

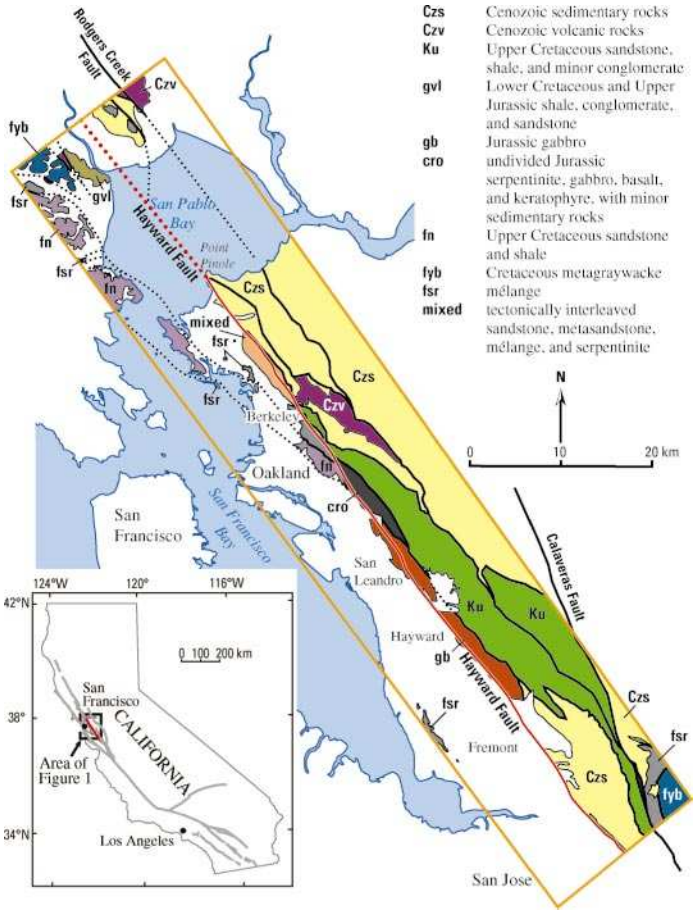

Figure 1. Location of study area and simple geologic map of Hayward fault zone within outline of three-dimensional geologic model (from Blake et al., 2002; Graymer, 2000; Graymer et al., 1996, 2002a; Wentworth et al., 1998; thick lines represent faults, dotted where concealed or inferred; Hayward fault in red).

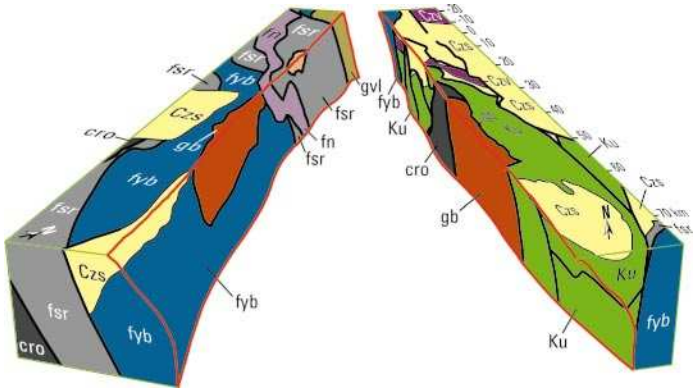

Figure 2. Oblique view of three-dimensional geologic map of Hayward fault zone (water and surficial deposits removed) split open to show fault faces (units as in Fig. 1; numeric scale on right is kilometers measured from Point Pinole).

The upper part of the active Hayward fault is within the gabbro body, with only ~5 km of right-lateral offset (Graymer, 1999). Similarly, a Tertiary mafic volcanic body was projected into the 3-D map volume (Czv in Fig. 3A) from the outcrop area of the volcanic rock farther north on the basis of its aeromagnetic signature and seismic reflection profiles and geologic cross sections (Wright and Smith, 1992). The upper traces of the contacts between some of the Franciscan Complex terranes, obscured by Quaternary deposits in the San Francisco Bay plain, were mapped on the basis of their gravity and magnetic signatures. The 3-D distribution of low-density Cenozoic deposits was quantitatively estimated by the inversion of gravity data (Jachens and Moring, 1990), which generated a surface representing the top of the Mesozoic basement for the southwestern half of the model.

Geologic Data

The remainder of the 3-D geologic map is based on the projection of surface geologic map information into the subsurface. Geologic units were generalized from Graymer (2000) on the basis of broad associations of age and lithology. Subsidiary faults were projected into the subsurface by applying a constant dip angle along their surface or concealed trace. Dip angles on some Franciscan terrane-bounding faults were extrapolated into the study area from observations to the northwest, where Mesozoic rocks are better exposed.

The 3-D map volume is divided by faults into 36 structural blocks based on a fault hierarchy derived from observed fault relationships and knowledge of recency of fault activity. The primary fault surface is the active Hayward fault, followed by other faults within the Hayward fault zone, and finally Mesozoic terrane-bounding faults.

Structural blocks are further divided by depositional contacts. In the preliminary map the main contacts are at the base of Quaternary surficial deposits, too thin to show at the scale of the figures, and at the base of Cenozoic deposits. Structural blocks at the north end of the map volume contain two additional contacts bounding the previously mentioned Tertiary volcanic body (Czv).

The intersection of the active Hayward fault with the adjacent faults, contacts, and rock bodies was then used to produce geologic maps of the east and west faces of the Hayward fault (Figs. 3A, 3B). The two geologic maps of the fault faces were also superposed to show rock units facing each other across the fault (Fig. 3D).

CORRELATION WITH FAULT BEHAVIOR

Several correlations between the geologic maps of the fault faces and fault behavior are observed (Figs. 3D–3G). The area of the west face occupied by Franciscan melánge (fsr) is characterized by much less seismicity than the remainder of the fault (feature 1 in Fig. 3F). There is a prominent cluster of seismicity around the contact between mélange and bedded sandstone (fn) in the western face of the fault, and another two around the contact between gabbro (gb) and metagraywacke (fyb) in the west face (Fig. 3F, features 2–4). There also is a fourth cluster of seismicity near the contact between ophiolitic rocks (cro) and Upper Cretaceous sandstone and shale (Ku) (Fig. 3E, feature 5). These relations suggest that seismicity correlates with rocks units and contacts on one side of the fault or the other, rather than rock interactions across the fault.

Waldhauser and Ellsworth (2002) used gaps in seismicity along the active fault to define locked patches at depth. The largest of the inferred locked patches, along with two others (Fig. 3F, features 6–8), is adjacent to Franciscan metagraywacke (fyb) on the west face. Waldhauser and Ellsworth (2002) defined a fourth patch (Fig. 3E, feature 9a–b) that does not correlate well with our maps. However, a significant number of hypocenters plot within their patch (part of the cluster near Berkeley, Fig. 3E, feature 5), which could divide the patch into two smaller areas, one entirely adjacent to Upper Cretaceous sandstone and shale (Ku; feature 9a) in the east face, the other (feature 9b) adjacent to the metagraywacke (fyb) in the west face, like features 6–8.

Over much of the fault length, surface creep rates are relatively uniform, with an average value of ~5.0 mm/yr and a range of 4.0–5.9 mm/yr (Fig. 3G, feature 10). An anomalously low creep rate of ~3.7 mm/yr occurs near Oakland (Fig. 3G, feature 11), where bedded sandstone (fn) and metagraywacke (fyb) together make a salient toward the surface.

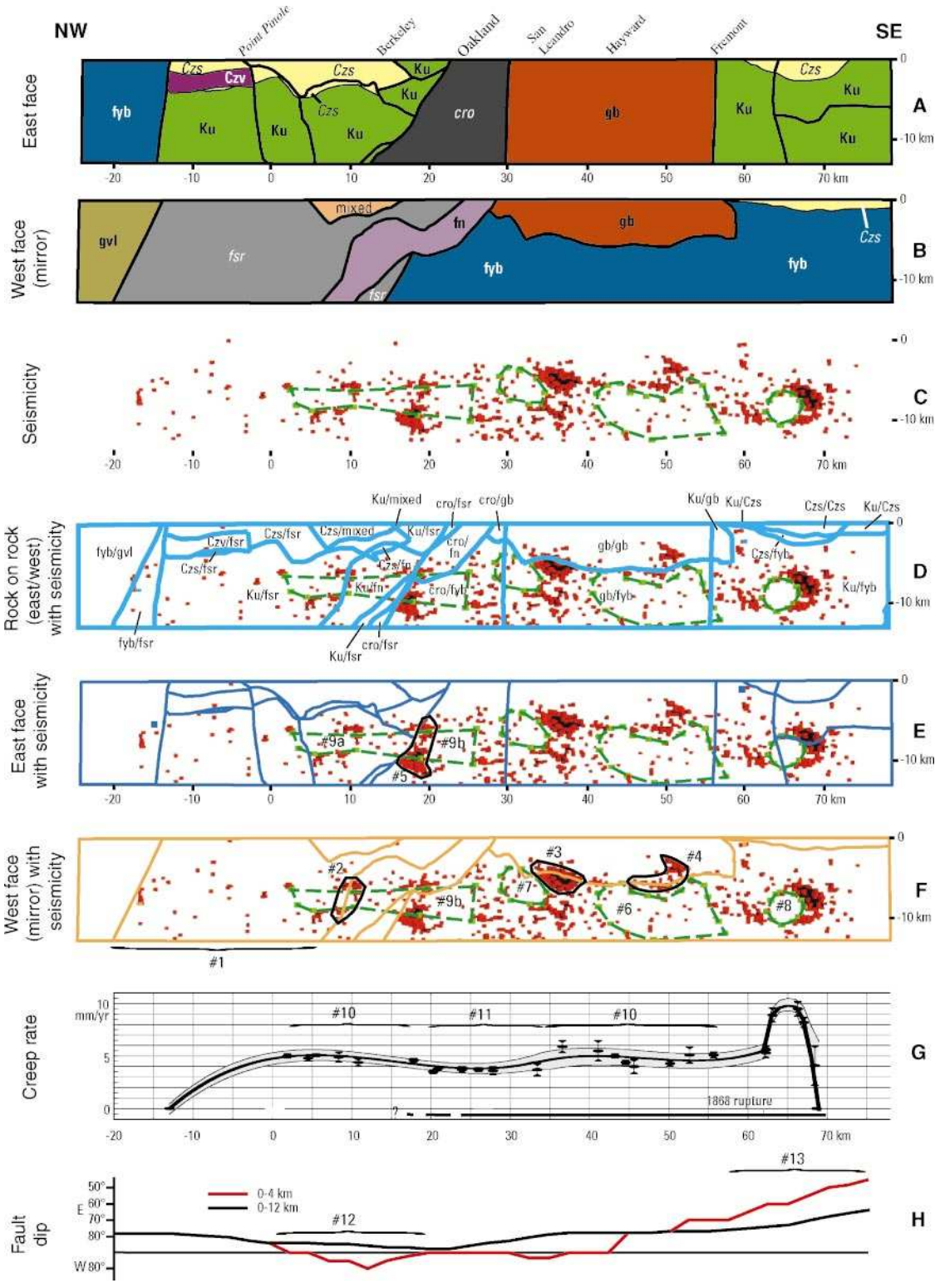

Figure 3. Fault-surface maps. Features discussed in text are numbered in black (features 1–13). A and B: East and west faces of Hayward fault (horizontal scale is in kilometers measured from Point Pinole; relatively strong units are labeled in bold, weak units in italics). C: Seismicity (from Waldhauser and Ellsworth, 2002; squares are double-difference hypocenters within 3 km of fault surface; green lines outline aseismic [possibly locked] patches). D: Rock-on-rock map with seismicity, showing rock types that are adjacent and presumably sliding past one another (first unit = east face; second unit = west face). Units as in Figure 1. E: East face geology with seismicity. F: West face geology with seismicity. G: Distribution of creep rate (Lienkaemper et al., 2001). H: Variation in fault dip (black line is average fault dip; red line is average fault dip in upper 4 km).

As modeled, the Hayward fault varies in dip along strike (Fig. 3H). Some changes in fault geometry correlate to changes in rock type along strike. For example, between Point Pinole and Berkeley, Cenozoic sedimentary rocks (Czs) in the upper 4 km of the east face correlate with west dips in the upper 4 km of the fault in contrast to the steep east dip of the fault zone as a whole (Fig. 3H, feature 12). The fault south of the gabbro (gb) is characterized by shallow dips in the upper 4 km and steep dips below (Fig. 3H, feature 13). Thus, the 3-D geometry of the fault surface may be affected by rock units adjacent to it.

Rock strength may play an important role in determining fault behavior. Laboratory measurements made on rock samples from the Hayward fault zone by Morrow and Lockner (2001) (Fig. 4A) are augmented with field observations by Ellen and Wentworth (1995) of hardness and fracture spacing, which may serve as a proxy for rock strength in units where direct measurements have not been made (Fig. 4B). Together, these data indicate that the three weakest units in the 3-D geologic map of the Hayward fault are Franciscan melánge (fsr), altered rocks of the Coast Range ophiolite (cro), and Cenozoic sedimentary rocks (Czs), whereas the strongest include bedded sandstone (fn,

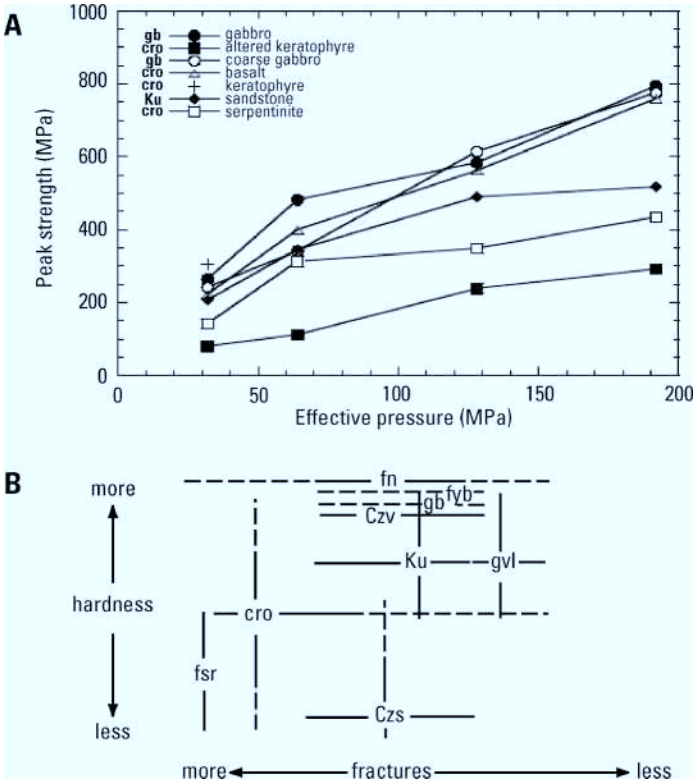

Figure 4. A: Rock strength (Morrow and Lockner, 2001) for Hayward fault samples. B: Field observations of hardness and fracture spacing (modified from Ellen and Wentworth, 1995; dashed lines indicate subordinate ranges) as indicator of rock strength, for geologic units in three-dimensional geologic map (explanation in Fig. 1). Note that unit cro includes variety of rock types (keratophyre, basalt, serpentinite).

Ku), metagraywacke (fyb), and gabbro (gb). Figure DR1[1] shows the relations between rock unit strength and fault behavior in more detail.

CONCLUSIONS

Possible relationships between fault behavior and geology along the Hayward fault are revealed in our 3-D geologic map of the fault and surrounding regions. Seismic and aseismic behavior as well as shape of the fault seem to correlate better with the extent of rock units or the location of their contacts as they abut the fault, rather than with variations in rock-body juxtapositions across the fault. This correlation may be related to the strengths of the rock units.

However, our 3-D model is still in its infancy, and we have identified steps to improve it. The inferred subsurface distribution of rock units needs to be tested with 3-D seismic tomography. The locations of some contacts on the fault faces may be sensitive to the inferred geometry, although simple tests with modest variations of fault dip suggest that the results shown in Figure 3 are robust. Nevertheless, additional tests are needed to explore the sensitivity of the results to model assumptions and to potential errors in the data sets used to construct the model. Similar studies should be undertaken on other faults to ascertain whether the relationships proposed for the Hayward fault can be observed elsewhere, as well as to expand our understanding of the role that rock properties play in fault behavior.

[1]GSA Data Repository item 2005096, Table DR1 (detailed description of rock unit to fault behavior relations) and Figure DR1 (rock strength compared to fault behavior), is available online at www.geosociety.org/pubs/ft2005.htm, or on request from editing@geosociety.org or Documents Secretary, GSA, P.O. Box 9140, Boulder, CO 80301-9140, USA.

REFERENCES CITED

Blake, M.C., Jr., Graymer, R.W., and Stamski, R.E., 2002, Geologic map and map database of western Sonoma, northern Marin, and southern Mendocino Counties, California: U.S. Geological Survey Miscellaneous Field Studies Map MF-2402, 42 p., scale 1:100,000.

Ellen, S.D., and Wentworth, C.M., 1995, Hillside materials and slopes of the San Francisco Bay region, California: U.S. Geological Survey Professional Paper P1357, 215 p.

Gilmore, T.D., 1992, Historical uplift measured across the eastern San Francisco Bay region, *in* Borchardt, G., et al., eds., Proceedings of the Second Conference on Earthquake Hazards in the Eastern San Francisco Bay Area: California Division of Mines and Geology Special Publication 113, p. 55–62.

Graymer, R.W., 1999, Offset history of the Hayward fault zone, San Francisco Bay region, California: Geological Society of America Abstracts with Programs, v. 36, no. 6, p. 59.

Graymer, R.W., 2000, Geologic map and map database of the Oakland metropolitan area, Alameda, Contra Costa, and San Francisco Counties, California: U.S. Geological Survey Miscellaneous Field Studies Map MF-2342, 29 p., scale 1:50,000.

Graymer, R.W., Jones, D.L., and Brabb, E.E., 1995, Geologic map of the Hayward Fault zone, Contra Costa, Alameda, and Santa Clara Counties, California: A digital database: U.S. Geological Survey Open-File Report 95–597.

Graymer, R.W., Jones, D.L., and Brabb, E.E., 1996, Preliminary geologic map emphasizing bedrock formations in Alameda County, California: A digital database: U.S. Geological Survey Open-File Report 96-252, 33 p., scale 1:75,000.

Graymer, R.W., Jones, D.L., and Brabb, E.E., 2002a, Geologic map database of northeastern San Francisco Bay region, California: U.S. Geological Survey Miscellaneous Field Studies Map MF-2403, 28 p., scale 1:100,000.

Graymer, R.W., Sarna-Wojcicki, A.M., Walker, J.P., McLaughlin, R.J., and Fleck, R.J., 2002b, Controls on timing and amount of right-lateral offset on the East Bay fault system, San Francisco Bay region, California: Geological Society of America Bulletin, v. 114, p. 1471–1479.

Jachens, R.C., and Moring, B.C., 1990, Maps of the thickness of Cenozoic deposits and the isostatic residual gravity over basement for Nevada: U.S. Geological Survey Open-File Report 90-404, 15 p., scale 1:1,000,000.

Kelson, K.I., and Simpson, G.D., 1995, Late Quaternary deformation of the southern East Bay Hills, Alameda County, CA: American Association of Petroleum Geologists Bulletin, v. 79, p. 590.

Lienkaemper, J.J., 1992, Map of recently active traces of the Hayward Fault, Alameda and Contra Costa Counties, California: U.S. Geological Survey Miscellaneous Field Studies Map MF-2196, 13 p., scale 1:24,000.

Lienkaemper, J.J., and Borchardt, G., 1996, Holocene slip rate of the Hayward Fault at Union City, California: Journal of Geophysical Research, v. 101B, p. 6099–6108.

Lienkaemper, J.J., Galehouse, J.S., and Simpson, R.W., 2001, Long-term monitoring of creep rate along the Hayward Fault and evidence for a lasting creep response to 1989 Loma Prieta earthquake: Geophysical Research Letters, v. 28, p. 2265–2268.

Morrow, C.A., and Lockner, D.A., 2001, Hayward Fault rocks: Porosity, density, and strength measurements: U.S. Geological Survey Open-File Report 01-421, 28 p.

Ponce, D.A., Hildenbrand, T.G., and Jachens, R.C., 2003, Gravity and magnetic expression of the San Leandro gabbro with implications for the geometry and evolution of the Hayward Fault zone, northern California: Seismological Society of America Bulletin, v. 93, p. 14–26.

Ponce, D.A., Simpson, R.W., Graymer, R.W., and Jachens, R.C., 2004, Gravity, magnetic, and seismicity profiles suggest a connection between the Hayward and Calaveras faults, northern California: Geochemistry, Geophysics, Geosystems, v. 5, no. 1, 39 p.

Sibson, R.H., 2003, Thickness of the seismic slip zone: Seismological Society of America Bulletin, v. 93, p. 1169–1178.

Waldhauser, F., and Ellsworth, W.L., 2002, Fault structure and mechanics of the Hayward Fault, California, from double-difference earthquake locations: Journal of Geophysical Research, v. 107B, p. 1–15.

Wentworth, C.M., Blake, M.C., Jr., McLaughlin, R.J., and Graymer, R.W., 1998, Preliminary geologic map of the San Jose 30 × 60 minute quadrangle, California: A digital map image: U.S. Geological Survey Open-File Report 98-795, 47 p., scale 1:100,000.

Working Group on California Earthquake Probabilities, 2003, Earthquake probabilities in the San Francisco Bay region: 2002–2031: U.S. Geological Survey Open-File Report 03-214, 235 p.

Wright, T.L., and Smith, N., 1992, Right step from the Hayward Fault to the Rodgers Creek Fault beneath San Pablo Bay, *in* Borchardt, G., et al., eds., Proceedings of the Second Conference on Earthquake Hazards in the Eastern San Francisco Bay Area: California Division of Mines and Geology Special Publication 113, p. 407–417.

Manuscript received 9 December 2004
Revised manuscript received 11 February 2005
Manuscript accepted 21 February 2005

Printed in USA

TABLE DR1. DETAILED DESCRIPTION OF ROCK UNIT TO FAULT BEHAVIOR RELATIONS

Relation number	Detailed description
#1	A distinctive drop in the amount of seismicity in the region where the west face is made up of mélange (fsr) northwest of about the 5 km mark. This seismicity drop does not correlate well with the east face because the unit at seismogenic depth there (Ku) is continuous into an area of increased seismicity to the south
#2	Two small clusters of seismicity at the contact between bedded sandstone (fn) and mélange in the west face. Note that seismicity is present above and below the aseismic patch (#9a). We correlate the seismic cluster with the west face, but the aseismic patch with the east face, suggesting the intersection may be an area of the fault where rock properties on either side of the fault are promoting different behavior
#3	A large cluster of seismicity at the contact between gabbro (gb) and metagraywacke (fyb) in the west face
#4	A cluster of seismicity at the contact between gabbro (gb) and metagraywacke (fyb) in the west face
#5	A large cluster of seismicity at the contact between ophiolite (cro) and bedded sandstone (Ku) in the east face. We suggest that this cluster divides the aseismic patch proposed by Waldhauser and Ellsworth (2002) into two smaller patches (#9a and #9b). Together with #2-4, these clusters suggest a concentration of strain at the contact between rock units in one fault face or the other
#6-#9	Aseismic (possibly locked) patches of Waldhauser and Ellsworth (2002). We suggest that their northernmost patch is subdivided by the seismic cluster near the 20 km mark (#5) into two separate patches we label #9a and #9b. We correlate #6, #7, #8, and #9b with the extent of metagraywacke (fyb) in the west face, and #9a with the extent of bedded sandstone (Ku) in the east face. It would be possible to correlate #6 and #7 with gabbro (gb), #8 with bedded sandstone (Ku), and #9b with ophiolite (cro) in the east face, but taken together all four make a more appealing coherent correlation with the west face. #9a does not correlate well with the west face as it crosses three rock units
#10	Along most of the fault, the surface creep rate is relatively uniform at about 5 mm/yr. Note that north of Point Pinole the fault is under the waters of San Pablo Bay, so surface creep cannot be detected or measured. The anomalously high rates south of the 62 km mark have not been explained, although they correlate pretty well with fault intersections in the east face
#11	A stretch of anomalously low creep rate between the 20-35 km marks is correlated with the upward salient of metagraywacke (fyb) and bedded sandstone (fn) in the west face
#12	The upper 4 km of the active fault dips west between about the 0-20 km marks, whereas the fault as a whole dips steeply east. We correlate this with the presence of Cenozoic sedimentary rocks (Czs) in the upper 4 km of the east face in that fault stretch
#13	The upper 4 km of the active fault dips east as shallowly as 50° south of the 55 km mark, whereas the fault as a whole dips steeply east. We correlate this with the southward transition from gabbro (gb) on both sides of the fault in the upper 4 km

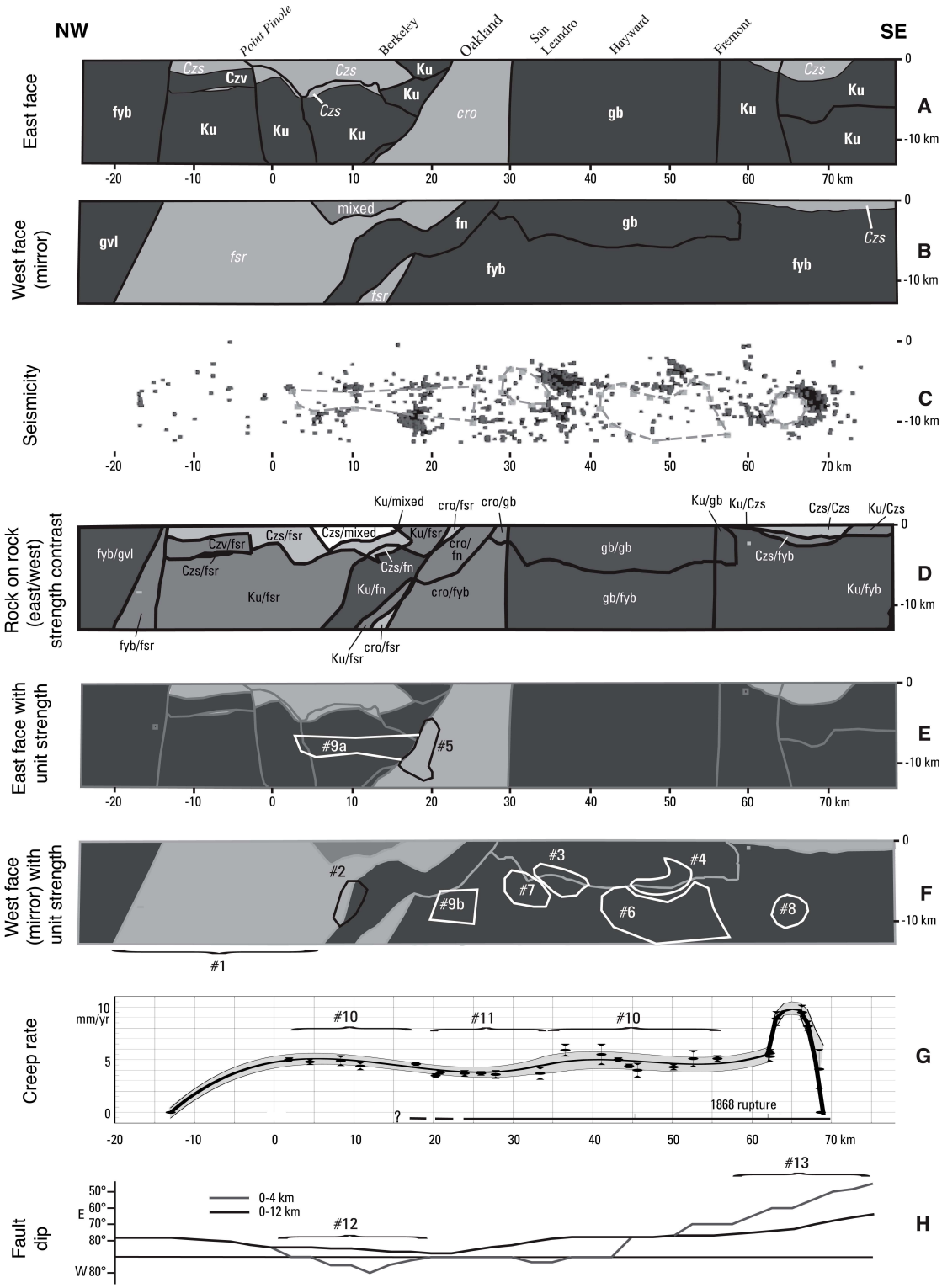

Figure DR1. Fault-surface maps emphasizing relative rock unit strength. Features discussed in text are numbered in black or white (features 1–13). Units as in Fig. 1. A and B: East and west faces of HF (horizontal scale is in kilometers measured from Point Pinole; relatively strong units are dark and labeled in bold, weak units are light and labeled in italics, the mixed unit is medium gray). C: Seismicity (from Waldhauser and Ellsworth, 2002; squares are double-difference hypocenters within 3 km of fault surface; lines outline aseismic [locked] patches). D: Rock-on-rock map, showing the strength contrast of rock units that are adjacent and presumably sliding past one another (first unit/second unit = east face/west face; strong/strong = dark gray, strong/weak or weak/strong = medium gray, weak/weak = light gray). E: East face geology with unit strength and fault behavior relations. F: West face geology with unit strength and fault behavior relations. G: Distribution of creep rate (Lienkaemper et al., 2001). H: Variation in fault dip (black line is average fault dip; light gray line is average fault dip in upper 4 km).